



Research Article

The Influence of Bonding Variations on Polymerization Shrinkage and Stress Distribution in Resin Composites: A Finite Element Comparative Study

Saiful Islam Izra'ai¹, Abdul Halim Abdullah^{1*}, Siti Mariam Ab Ghani², Amir Radzi Ab Ghani¹

¹School of Mechanical Engineering, College of Engineering, Universiti Teknologi MARA, 40450 Shah Alam, Selangor, Malaysia

²Center for Restorative Dentistry Studies, Faculty of Dentistry, Universiti Teknologi MARA, Sungai Buloh Campus, 47000 Sungai Buloh, Selangor, Malaysia

*Corresponding author: halim471@uitm.edu.my; Tel.: +60355436468; Fax: +60355435160

Abstract: This study aimed to investigate the biomechanical behavior of Class I resin composite restorations under varying bonding conditions using finite element analysis (FEA). Despite offering aesthetic and functional benefits, resin-based composites are susceptible to polymerization shrinkage, leading to internal stresses that may compromise restoration longevity. Four finite element models were developed, namely Model A (fully bonded), Model B (single-wall debonded), Model C (adjacent walls debonded), and Model D (opposite walls debonded). The analysis showed that debonding configurations significantly influenced volume displacement, linear displacement, and stress distribution. Debonded models showed higher volume displacements, with Model C having the most significant increase. Despite reducing vertical displacements, these models had higher localized stress concentrations compared to fully bonded. In conclusion, surface measurements could serve as a non-invasive method for detecting subsurface debonding, offering valuable insights into stress patterns that could impact the durability of composite restorations.

Keywords: Dental restorations; Finite Element Analysis (FEA); Polymerization shrinkage

1. Introduction

Resin-based composites have revolutionized restorative dentistry over the past several decades, particularly in Class I and II restorations. Initially developed to restore the aesthetics and function of human dentition, these materials have become the preferred choice for many dental professionals due to the ability to closely mimic the natural appearance of tooth while providing functional durability (Melo et al., 2023; Ab Ghani et al., 2022; Hamdy, 2021; Heck et al., 2018). Despite the widespread use, the clinical success and longevity of resin-based composite restorations depend on numerous factors, including material properties, the bioactivity of resin, patient-specific variables such as oral health compliance, and the operator's skill during the restorative procedure (Genisa et al., 2020; Pereira et al., 2020; Ausiello et al., 2019; Moraschini et al., 2015; Magne, 2007).

This work was supported by the Faculty of Dentistry and School of Engineering, Universiti Teknologi MARA (Malaysia), funded by the Fundamental Research Grant Scheme, reference number 600-IRMI/FRGS5/3(030/2019), provided by the Ministry of Higher Education (Malaysia)

<https://doi.org/10.14716/ijtech.v16i2.7357>

Received September 2024; Revised November 2024; Accepted January 2025

One of the most significant challenges associated with resin-based composites is the inherent tendency to undergo volumetric polymerization shrinkage, which can range from 1% to 4.8%, depending on various chemical and physical factors (Gallo et al., 2019; Al Sunbul et al., 2016; Martinsen et al., 2013; Nagem Filho et al., 2007). These factors include the presence and concentration of dimethacrylate matrix monomers and the volume percentage of inorganic filler within the composite (Avcılar and Bakır, 2023; Ersen et al., 2020). Polymerization shrinkage is intrinsically related to the generation of shrinkage stress, influenced not only by the composite's material properties, such as its Young's modulus, but also by the cavity geometry, boundary conditions, and the stiffness of the remaining tooth structure (Algamaiah et al., 2021; Dejak and Młotkowski, 2015; Kim et al., 2015; Weinmann et al., 2005). In adhesively restored Class I cavities, shrinkage stress exerts internal and marginal forces that increase the risk of failure by creating debond gaps at tooth-restoration interface (Ferracane and Hilton, 2016; Ferracane, 2005).

The primary source of stress in a restored tooth typically arises from dimensional changes in the composite material at tooth-restoration interface or from occlusal loads exerted on the restoration during function (Anhesini et al., 2019; Fennis et al., 2005). These phenomena have been extensively studied through both laboratory experiments and finite element analysis (FEA), providing valuable insights into the behaviour of composite materials under various clinical conditions (Ab Ghani et al., 2023; Nayak et al., 2021; Ausiello et al., 2019; 2017a; 2017b; Chuang et al., 2011). However, the complex interactions between polymerization shrinkage strain, stress, elastic modulus, and adhesive bonding at the restoration margins continue to pose significant challenges in achieving optimal clinical outcomes.

Marginal adaptation of restorations in bonded dentin cavities reflects a delicate balance between these factors. Shrinkage stress and the potential for debonding are significantly influenced by the cavity shape and constraints, the interface bond strength, and the degree of conversion (DC) of the composite material, which depends on the effectiveness of light-curing (Soares et al., 2017; Wang and Chiang, 2016). In deep Class I restorations with high C-factor, polymerization shrinkage directs stress centrally, raising the risk of interface debonding and microleakage if stresses exceed resin-dentin bond strength (Soares et al., 2017; Chuang et al., 2011; Versluis et al., 2004). Currently, bulk-fill dental composites have the potential to address some of these limitations (Albeshir et al., 2022; Sampaio et al., 2019). Studies have shown that the displacement of resin composite restorations due to polymerization shrinkage is closely tied to the integrity of bonding at cavity surfaces.

This study introduced a novel method for detecting subsurface debonding in resin-based composites by using occlusal surface displacement measurements, providing a non-invasive alternative to traditional X-ray imaging. In addition, it incorporates advanced FEA to evaluate the relationship between polymerization shrinkage, stress distribution, and different bonding conditions under clinically relevant scenarios. The study specifically addressed the gap in understanding how various bonding conditions in Class I restoration influenced shrinkage stress and debonding risks. Unlike previous studies, it expanded the scope by incorporating more bonding conditions, surface displacement measurements, and advanced simulation methods to enable more accurate predictions of debonding risks and restoration failure. By addressing these challenges, the longevity and effectiveness of resin-based composite restoration in clinical practice can be improved.

2. Materials and Methods

This study developed and validated a detailed 3D CAD model of Class I dental restoration based on (Ab Ghani et al., 2023). The in-vitro experimental setup used micro-CT imaging to measure volume changes in fully bonded restorations due to polymerization. Class I cavities (4×4×4 mm³) were prepared in ten sound molars, etched with 37% phosphoric acid, and bonded using Optibond FL®, followed by the placement of Filtek™ Bulk Fill composite. Subsequently, specimens were light-cured for 20 seconds and scanned pre- and post-polymerization using micro-CT, with consistent positioning ensured by embedding roots in acrylic holders. 3D models were

reconstructed using CT Pro 3D and analyzed in ImageJ to visualize displacement patterns through image subtraction. Volumetric changes at the surface and base were quantified using CTAnalyzer, with a region of interest (ROI) and binarization applied for precise measurements. These results provided experimental validation for FEA predictions of polymerization shrinkage.

Biomechanical responses in dental applications have been extensively analyzed using advanced CAD-FEM (Computer Aided Design and Finite Element Method) (Siripath et al., 2024; Norli et al., 2024; Ab Ghani et al., 2023; Nayak et al., 2021; Ahmad et al., 2020; Ismail et al., 2020; Novaes et al., 2018; Ausiello et al., 2017a; 2017b). FEA of Class I restoration model was conducted using ABAQUS 6.13 (SIMULIA, Dassault Systèmes, Providence, RI, USA). The model included precise dimensions, namely 10.5×12.4×7.8 mm for the tooth, 4×4×4 mm for resin composite, and a 10 µm thick adhesive layer as shown in Figure 2. The restoration was oriented with the x-axis representing the facial-lingual direction, the z-axis the mesial-distal direction, and the y-axis the axial direction. Meanwhile, the meshing process utilized 8-node linear brick elements, specifically linear hexahedral elements, with three degrees of freedom per node. The specific number of elements and nodes used in the model is detailed in Table 1.

Table 1 Technical features of tooth model

Component	Total number of elements	Total number of nodes	Total of degrees of freedom
Adhesive	540	1122	3,366
Dentine	15765	17810	53,430
Enamel	2375	3246	9,738
Resin Composite	8000	9261	27,783

2.1. Model Development

Based on the 3D CAD model, four different bonding conditions, labeled A, B, C, and D were developed and analyzed to examine the impact on the stress distribution and volume displacement of resin composite. The specifics of these conditions, along with bonding characteristics, are presented in Figure 1.

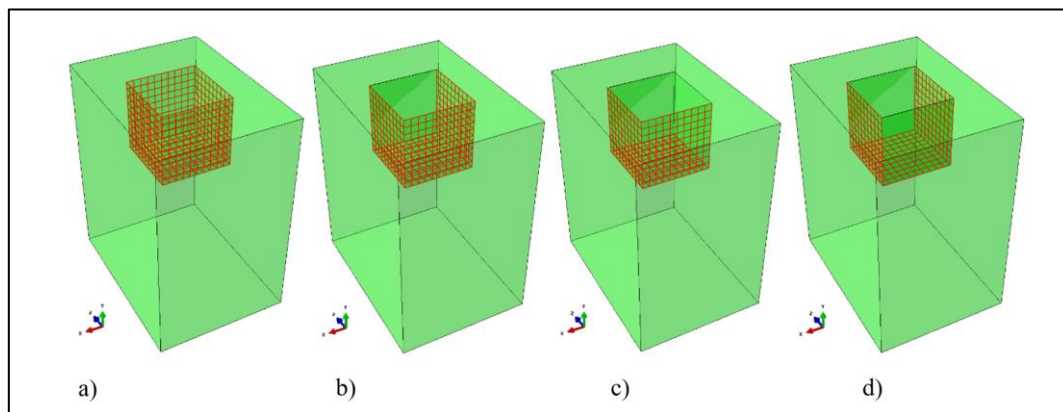


Figure 1 Bonding characteristics of the composite: a) all walls bonded, b) one wall debonded, c) one wall and its adjacent wall debonded, d) one wall and its opposite wall debonded

Model A, where all walls are bonded; Model B, where one wall is debonded; Model C, where one wall and its adjacent wall are debonded; and Model D, where one wall and its opposite wall are debonded. These conditions were validated against Ab Ghani's work on fully bonded models. The bottom surface of the tooth model was constrained to have zero displacements in all three directions (encastre). A tie constraint was applied to the contact surfaces between the dentine, enamel, resin, and composite for each model part, with the exception of the cavity floor and the

restoration base in debonded conditions, which were separated to simulate debonding, as presented in Figure 3. Furthermore, the mechanical properties of three dental materials, namely enamel, dentine, and adhesive, were incorporated into the analysis. Enamel is characterized by a Young's modulus of 80,000 MPa and a Poisson's ratio of 0.33. Dentine, with a Young's modulus of 19,000 MPa, shares the same Poisson's ratio of 0.33. In contrast, the adhesive material has a lower Young's modulus of 1,000 MPa and a Poisson's ratio of 0.3 (Ab Ghani et al., 2023; Novaes et al., 2018).

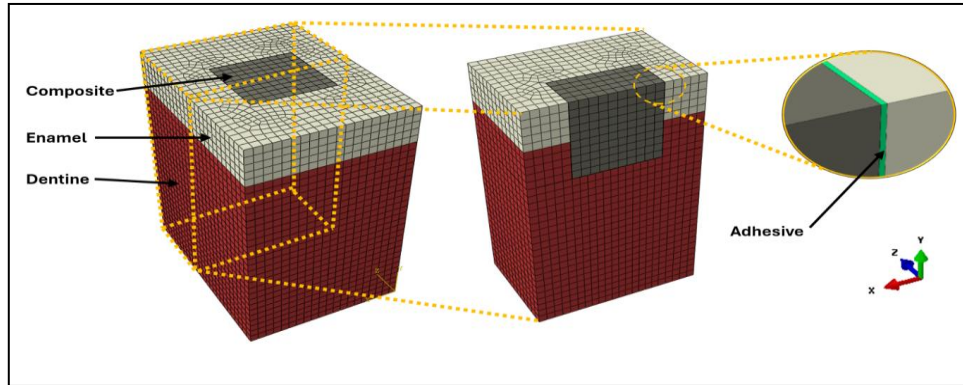


Figure 2 3D FE model: a) tooth structure (enamel and dentine), resin composite, and adhesive layer, b) mesial-distal cut section at the centre of the model, and c) 10 µm thick adhesive layer

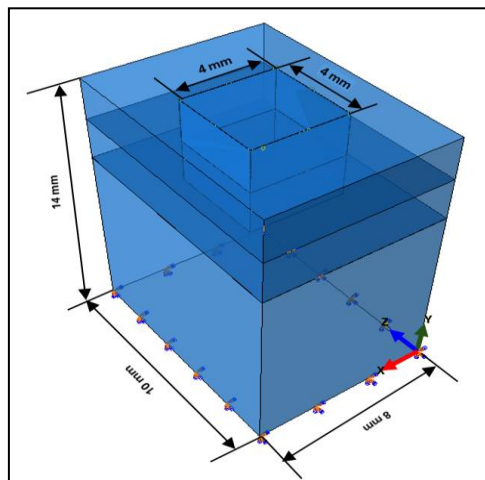


Figure 3 Schematic Diagram Illustrating the Geometry of the Model Restoration and Constraint Conditions of the Finite Element Model

2.2. Polymerization Shrinkage Simulation

A pseudo-coefficient of thermal expansion (α) was defined by the equation $\Delta\epsilon_s = \alpha\Delta T$, where ΔT represents the change in temperature to simulate polymerization shrinkage in resin composite. The temperature was assumed to increase linearly over time at 1:1 ratio, providing a simplified but realistic simulation of thermal effects during the curing process. This simulation was implemented through predefined fields assigned to resin composite, allowing for different amplitudes of temperature change at each step to account for localized variations in thermal behavior. The curing process was divided into seven discrete steps over a total duration of 85 seconds, with each step representing a specific phase of temperature and mechanical property evolution. Initially, resin composite showed a Young's modulus (E) of 0.027 GPa in its uncured state, which progressively increased to 12 GPa by the end of the curing process. Both the pseudo-coefficient of thermal expansion and the Young's modulus were treated as time-dependent parameters to accurately

capture the evolving material properties at each step. These values, detailed in Table 2, emphasized the dynamic changes in the composite's thermal and mechanical behavior, offering a comprehensive framework for analyzing polymerization process.

FEA was conducted on restored Models A, B, C, and D to evaluate vertical displacement and compare first principal stresses (MPa) along Path 1, located on the middle plane between the adhesive and composite resins, and Path 2, positioned along bonded facial wall. Stress distribution across these paths showed critical areas experiencing the highest stress concentrations, particularly in regions such as the enamel, dentin, and cavity floor.

The calculation of volume displacement due to polymerization shrinkage in resin composite restorations was conducted using Abaqus/CAE software. FEA was conducted under specified polymerization conditions, generating .odb files containing displacement field data. The initial volume of resin composite in its undeformed state, $V_{initial}$, was determined using the volume query tool in Abaqus Visualization module, applied to the simulation's initial frame where no deformation had occurred. Subsequently, the deformed volume, V_{final} , was calculated using the same query tool, focusing on the final frame of the simulation, where polymerization shrinkage was fully realized. The visualization of the displacement field facilitated precise identification of this final frame.

Table 2 Young's modulus and pseudo coefficient of thermal expansion of resin composite as a function of time for simulating shrinkage load in FEA (Ab Ghani et al., 2023; Novaes et al., 2018)

Step	t(s) = T(°C)	ΔT (°C)	E (MPa)	α (°C ⁻¹)
1	22.13	22.13	27.13	-0.00000555
2	26.03	3.9	268.49	-0.00000123
3	45.05	19.02	10514.55	-0.000000366
4	84.94	39.89	11991.74	-0.000000227
5	134.06	49.12	11999.45	-0.0000000707
6	308.46	174.40	11999.98	-0.0000000254
7	595.30	286.84	12000.00	-0.0000000123

The volume difference (ΔV) and the percentage shrinkage (%Shrinkage) were computed using manual equations to quantify the volume changes. The volume difference was calculated as $\Delta V = V_{final} - V_{initial}$, representing the net change in volume after polymerization. Meanwhile, the percentage shrinkage was determined using $\%Shrinkage = \left(\frac{\Delta V}{V_{initial}} \right) \times 100$, allowing for the evaluation of polymerization-induced shrinkage relative to the initial volume. These computations provided a comprehensive understanding of the material's volumetric response during polymerization process.

3. Results and Discussion

FEA conducted in this study provided valuable insights into how different bonding configurations affected polymerization shrinkage and stress distribution in Class I composite restorations. The results showed the significant impact of cavity wall bonding on the mechanical behavior of resin composites during polymerization, particularly in terms of displacement and stress concentration.

FEA was validated by comparing its results with fully bonded micro-CT measurements reported by Ab Ghani et al. (2023). The volume displacement recorded was 1.33 mm³, closely corresponding with the 1.36 ± 0.2 mm³ measured by micro-CT. Therefore, the model effectively captured polymerization-induced shrinkage effects observed experimentally. The vertical displacement predicted by the model was 59.95 μm, closely corresponding with the 62.5 ± 5.2 μm measured by micro-CT. This consistency in displacement values further supported the model's accuracy in

replicating the real-world behavior of resin composite restorations. The ability of FEA to predict both volumetric and vertical displacement with recorded precision emphasized the reliability and validity in modeling resin composite restorations under fully bonded conditions. These results confirmed the model served as a robust tool for understanding and optimizing dental restoration methods (Ab Ghani et al., 2023).

FEA was conducted on Models A, B, C, and D to evaluate the total displacement resulting from polymerization shrinkage, modeled as thermal expansion (α) in resin composite. Based on Figure 3, Model A, with all walls bonded, had the highest maximum displacement of 59.95 μm , concentrated at the center of the top surface. Model B, where one wall is debonded, showed a reduced maximum displacement of 33.32 μm , with deformation localized near debonded region. In Model C, where one wall and its adjacent wall were debonded, the maximum displacement further decreased to 27.42 μm , with displacement concentrated along debonded interface. Model D, where one wall and its opposite wall are debonded, had the lowest maximum displacement of 24.04 μm , with displacement symmetrically distributed along debonded walls. These results showed a trend of decreasing maximum displacement as more walls were debonded, with displacement becoming more localized around debonded areas in each successive model.

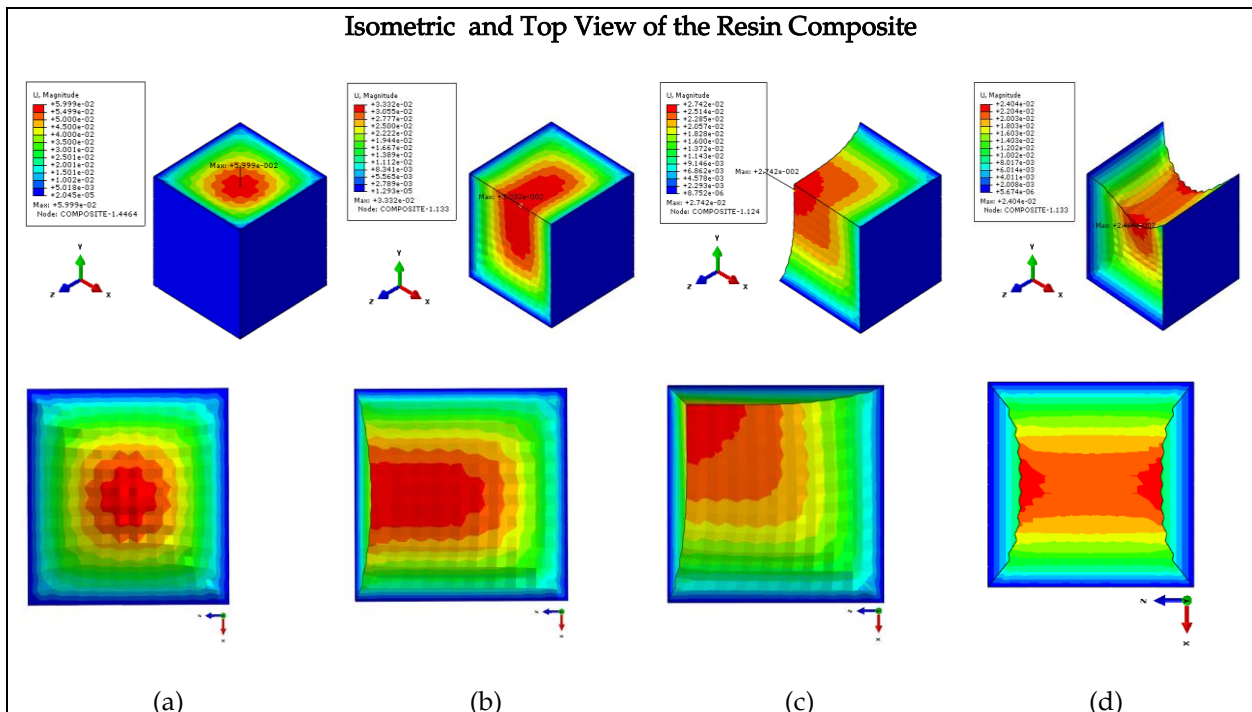


Figure 4 Overall contour plots of the total displacement for each analyzed models of resin composite: (a) Model A, (b) Model B, (c) Model C and (d) Model D in isometric view and top view

Based on Figure 4, fully bonded restorations (Model A) had the highest total displacement (59.95 μm) due to the constraint imposed on the composite by bonded cavity walls. This was consistent with previous studies, where complete bonding restricted the composite's ability to contract freely, leading to increased internal stresses and greater overall displacement (Gallo et al., 2019; Sampaio et al., 2019; Ferracane and Hilton, 2016). As bonding constraints were reduced in Models B, C, and D, total displacement decreased, with Model D showing the lowest displacement (24.04 μm). Although reducing bonding constraints could alleviate overall shrinkage displacement, it could also lead to more localized deformation, particularly around debonded regions. Clinically, while the risk of central cracking might be reduced, there could be an increased risk of marginal integrity issues, such as marginal gaps or microleakage, specifically at debonded interfaces.

Several studies have utilized Abaqus, incorporating subroutines and Python scripts, to calculate volume changes in various models by leveraging the output database (.odb) file for precise analysis. These studies showed the versatility of Abaqus in assessing volume changes and the resulting mechanical behavior in different materials and configurations (Kholil et al., 2023; Liu et al., 2017; Mokhatar and Abdullah, 2012). The analysis of volume displacement across the models supported the results related to stress distribution. Based on Figure 5, fully bonded restorations (Model A) had the lowest total volume displacement (1.36 mm^3), reflecting the restricted contraction of the composite material. However, Models B and C, featuring debonded walls, had higher volume displacement (1.94 mm^3 and 2.01 mm^3 , respectively), confirming that reduced bonding constraints allowed for greater material contraction at the risk of increased localized stress. According to this relationship, while debonding might reduce overall stress, it also permits greater freedom of movement for the material, potentially leading to weak points at the margins where stress could accumulate and cause long-term issues (Novaes et al., 2018; Rodrigues et al., 2012).

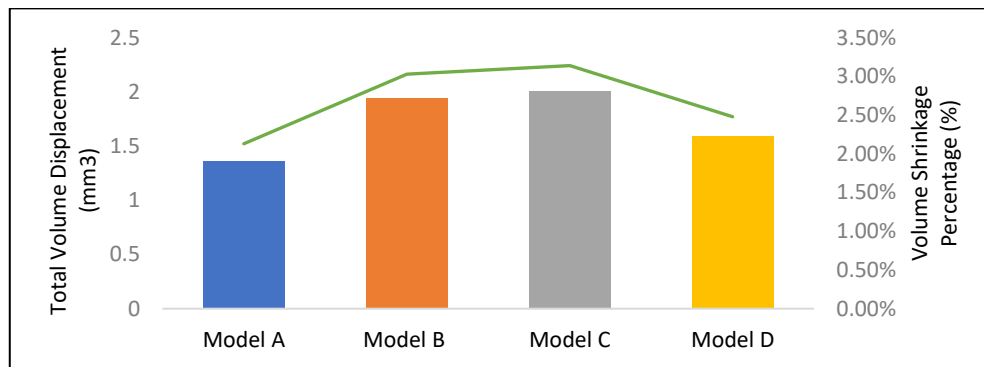


Figure 5 Comparison of Volume Displacement and Volume Shrinkage Percentage of Composite in Models A, B, C, and D

In Figure 6(a), FEA-predicted linear displacement along the horizontal occlusal surface of Models A, B, C, and D, from the mesial (0 mm) to the distal wall (4 mm), showed that Model A had the largest vertical displacement, with a maximum downward movement of $-59.95 \mu\text{m}$ occurring at 2.20 mm from the mesial wall. Model B, having one debonded wall, showed a reduced maximum displacement of $-32.89 \mu\text{m}$ at 0.16 mm, with a generally consistent displacement profile across the surface. Model C, characterized by adjacent wall debonding, further reduced the maximum displacement to $-22.75 \mu\text{m}$, also at 0.16 mm. Model D, with opposite walls debonded, showed the smallest vertical displacement, peaking at $-23.11 \mu\text{m}$ at the distal wall (4.00 mm).

Model A, representing a fully bonded restoration, had the highest vertical displacement, with a peak of $-59.95 \mu\text{m}$. The high vertical displacement in Model A showed that the secure bonding concentrated stress, specifically at the midpoint of the occlusal surface. As bonding imperfections were introduced in Models B, C, and D, vertical displacement decreased, with Model D (opposite walls debonded) showing the lowest displacement, as seen in Figures 6(a) and 6(b). Therefore, unintentional debonding allowed the composite to move more freely, reducing vertical stress concentration. The increased movement led to localized stress, potentially compromising the restoration's long-term durability, consistent with previous studies, where reducing bonding constraints could alleviate stress in some areas while introducing new stress points (Novaes et al., 2018, Ferracane and Hilton, 2016).

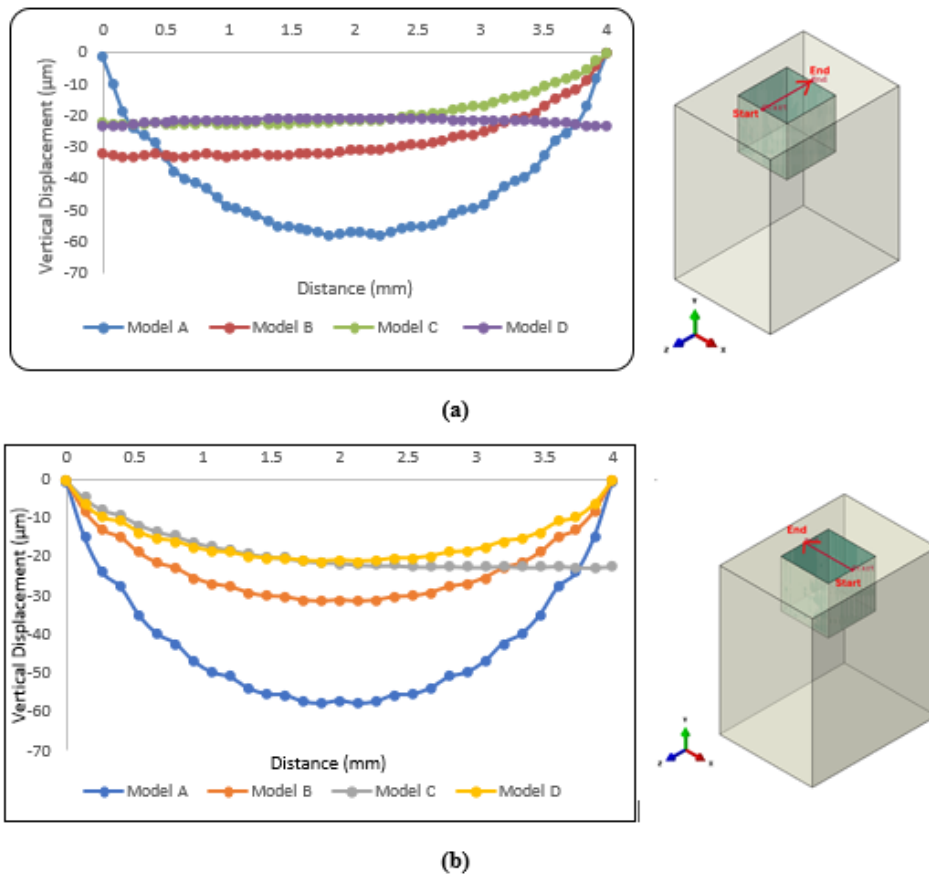


Figure 6 Comparison of FEA-predicted linear displacement along the horizontal occlusal surface for models A, B, C, and D, from the (a) mesial (0 mm) to the distal wall (4 mm), (b) facial (0 mm) to the lingual wall (4 mm)

The analysis showed a clear trend of decreasing maximum vertical displacement from Models A to D, with the most significant differences occurring near the mid-point (around 2 mm) and the distal wall (4 mm) along the occlusal surface. Similarly, in Figure 5(b), the FEA-predicted linear displacement from the facial (0 mm) to the lingual wall (4 mm) followed a comparable pattern. Model A also showed the largest displacement, with a maximum of $-59.95 \mu\text{m}$ near the mid-point, confirming significant shrinkage stress in fully bonded condition. Model B, with one debonded wall, had a lower maximum displacement of $-32.89 \mu\text{m}$, confirming partial stress relief. Model C, with adjacent wall debonding, further reduced this to $-22.75 \mu\text{m}$, while Model D, with opposite walls debonded, had the smallest displacement at $-23.11 \mu\text{m}$. This consistent reduction in vertical displacement with increasing debonding emphasized how debonding influenced stress distribution and the resulting displacement patterns across the restoration.

The relationship between vertical and volumetric displacement showed the significant impact of unintentional debonding on stress distribution in resin composite restorations. Fully bonded conditions, characterized by higher vertical displacement and lower total volume displacement, showed that polymerization shrinkage was confined to specific areas, leading to concentrated stress distribution (Antunes Junior et al., 2020; Fok and Chew, 2020; Boaro et al., 2010). However, configurations with partial debonding led to higher total volume displacement, confirming that the absence of bonding allowed for more uniform shrinkage across three dimensions. This uniformity reduced vertical movement but increased overall volumetric displacement and localized stress concentrations. The results showed that while debonding could mitigate localized vertical shrinkage, it amplified volumetric displacement, emphasizing the importance of maintaining bonding integrity to ensure the mechanical stability and longevity of dental restorations (Ab Ghani et al., 2023; Novaes et al., 2018).

Along Path 1 (Figure 7), lying on the middle plane between the adhesive and composite resins, restorations with fully bonded walls had the highest stress concentrations, particularly near the corners and junctions where the floor met the walls. Peak stress reached approximately 1.73 MPa, with high stress levels concentrated in the floor region between 4 mm and 8 mm, as well as marginal areas near the enamel and dentin. When a single wall was unintentionally debonded, stress levels decreased slightly, with peak stresses around 1.39 MPa at similar critical locations. Further reductions were observed when additional walls were debonded, either one wall and its adjacent wall or one wall and its opposite wall, resulting in maximum stresses of approximately 1.24 MPa and 0.71 MPa, respectively. Along Path 2 (Figure 8), running along bonded facial wall, a similar trend was observed. Fully bonded restorations had the highest stress levels, with peak stresses of about 1.73 MPa in the dentin regions and floor areas. As debonding increased, stress levels progressively decreased, with the lowest values observed in cases where multiple walls were debonded, reaching as low as 0.66 MPa. These results showed the significant influence of bonding conditions on stress distribution. Fully bonded restorations had higher overall stress but a more uniform distribution compared to partially debonded scenarios. In both Path 1 and 2, the highest stress concentrations occurred in critical areas such as corners, junctions, and cavity floor. As walls became unintentionally debonded, stress levels decreased, with the most uniform and lowest stress observed when multiple walls were debonded. This showed the crucial role of bonding conditions in determining stress distribution.

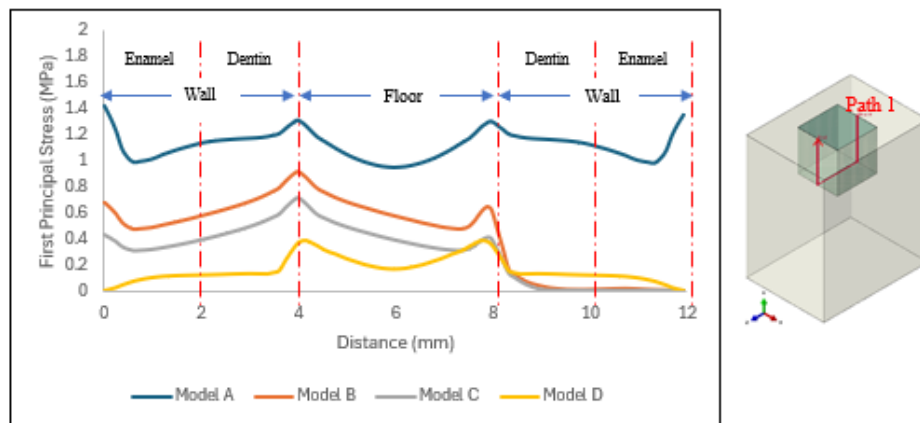


Figure 7 Comparison of First Principal Stresses (MPa) along inspection lines in restored model along Path 1

FEA showed that fully bonded configurations (Model A) had higher stress concentrations, particularly at critical areas such as the corners, junctions, and cavity floor. The stress hotspots corresponded to the rigidity of fully bonded restorations, restricting material shrinkage and direct stress toward these points (Fok and Chew, 2020; Boaro et al., 2010; Versluis et al., 2004). Stress distribution varied based on wall conditions, namely single-wall debonding concentrated stress near the detached surface, adjacent-wall debonding increased stress at the junctions of debonded walls, and opposite-wall debonding led to more even stress distribution but higher stress at the margins. Each debonding condition significantly influenced stress localization and distribution. Although debonding can alleviate overall stress, it might also introduce new stress concentrations that may compromise the restoration long-term performance (Algamaiah et al., 2017; Magne, 2007). The analysis of first principal stresses along Path 1 and Path 2 further reinforced the results, with critical stress concentrations occurring in areas essential for the mechanical integrity of the restoration, such as the junctions and floors (Ab Ghani et al., 2023; Krishna Alla et al., 2023).

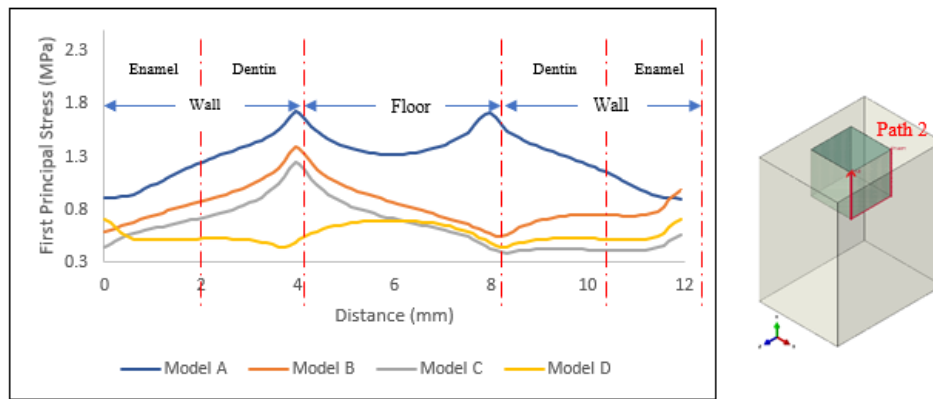


Figure 8 Comparison of First Principal Stresses (MPa) along inspection lines in restored model along Path 2

Conducted under controlled conditions, this study offered valuable insights into the biomechanical behavior of Class I composite restorations under different bonding configurations. However, real-world clinical settings introduced additional challenges, such as moisture, temperature fluctuations, and the complexity of tooth anatomy, potentially impacting restoration outcomes. Achieving complete bonding of all cavity walls was often difficult, leading to partial or irregular debonding patterns that influenced stress distribution and polymerization shrinkage unpredictably (Ersen et al., 2020; Novaes et al., 2018). To improve clinical relevance, further investigations using advanced imaging methods, such as optical coherence tomography (OCT), were recommended to assess subsurface defects in vivo, validate FEA results, and explore a broader range of debonding configurations. This current study showed the importance of careful bonding strategies during restorative procedures and the regular monitoring of restorations, specifically those with complex bonding conditions, to ensure long-term clinical success (Algamaiah et al., 2017).

4. Conclusions

In conclusion, this study showed the significant impact of bonding configurations on the biomechanical behavior of Class I resin composite restorations. FEA showed that while debonding reduced overall shrinkage-induced displacements, it increased localized stress concentrations, particularly in asymmetric debonding scenarios. Furthermore, the results showed that surface displacement measurements could serve as a non-invasive tool for detecting and monitoring subsurface debonding, improving the assessment and durability of composite restorations. This method had the potential to improve clinical outcomes by providing early insights into restoration integrity.

Acknowledgements

This study was funded by the Faculty of Dentistry, School of Engineering Universiti Teknologi MARA (Malaysia) and the Ministry of Higher Education (Malaysia) through the Fundamental Research Grant Scheme, reference number 600-IRMI/FRGS5/3(030/2019).

Author Contributions

S.I. Izra'ai and A.H. Abdullah designed the model and the computational framework and analyzed the data. S.I. Izra'ai developed the simulations, performed the calculations, analyzed the data, and wrote the manuscript. S.M. Ab Ghani performed experimental validation and provided expertise in dentistry-related aspects of the study. A.R. Ab Ghani assisted with simulation validation, provided professional engineering insight, and contributed to the manuscript preparation. All authors discussed the results, provided critical feedback, and contributed to the final manuscript.

Conflict of Interest

The authors declare no conflict of interest regarding the publication of this article.

References

- Ab Ghani, S, Tengku Mohd Ariff, T, Ong, T & Lim, T 2022, 'The implementation of the minimal intervention dentistry in the undergraduate dental clinical teaching: A retrospective audit', *Compendium of Oral Science*, vol. 9, no. 2, pp. 63-68, <https://doi.org/10.24191/cos.v9i2.19234>
- Ab Ghani, SM, Abu Hassan, MI, Abdullah, AH, Ab Ghani, AR, Izra'ai, SI, Aregawi, W, Chew, HP & Fok, A 2023, 'Linear and volumetric shrinkage displacements of resin composite restorations with and without debonding', *Dental Materials Journal*, vol. 42, no. 5, pp. 659-668, <https://doi.org/10.4012/dmj.2023-023>
- Ahmad, MA, Zulkifli, NNM, Shuib, S, Sulaiman, SH & Abdullah, AH 2020, 'Finite element analysis of proximal cement fixation in total hip arthroplasty', *International Journal of Technology*, vol. 11, no. 5, pp. 1046-1055, <https://doi.org/10.14716/ijtech.v11i5.4318>
- Al Sunbul, H, Silikas, N & Watts, DC 2016, 'Polymerization shrinkage kinetics and shrinkage-stress in dental resin-composites', *Dental Materials*, vol. 32, no. 8, pp. 998-1006, <https://doi.org/10.1016/j.dental.2016.05.006>
- Albeshir, EG, Alsaifi, R, Albluwi, R, Balhaddad, AA, Mitwalli, H, Oates, TW, Hack, GD, Sun, J, Weir, MD & Xu, HHK 2022, 'Low-shrinkage resin matrices in restorative dentistry: Narrative review', *Materials*, vol. 15, no. 8, pp. 1-21, <https://doi.org/10.3390/ma15082951>
- Algamaiah, H, Sampaio, CS, Rigo, LC, Janal, MN, Giannini, M, Bonfante, EA, Coelho, PG, Reis, AF & Hirata, R 2017, 'Microcomputed tomography evaluation of volumetric shrinkage of bulk-fill composites in class II cavities', *Journal of Esthetic and Restorative Dentistry*, vol. 29, no. 2, pp. 118-127, <https://doi.org/10.1111/jerd.12275>
- Algamaiah, H, Silikas, N & Watts, DC 2021, 'Polymerization shrinkage and shrinkage stress development in ultra-rapid photo-polymerized bulk fill resin composites', *Dental Materials*, vol. 37, no. 4, pp. 559-567, <https://doi.org/10.1016/j.dental.2021.02.012>
- Anhesini, BH, Landmayer, K, Nahsan, FPS, Pereira, JC, Honório, HM & Francisconi-dos-Rios, LF 2019, 'Composite vs. ionomer vs. mixed restoration of wedge-shaped dental cervical lesions: Marginal quality relative to eccentric occlusal loading', *Journal of the Mechanical Behavior of Biomedical Materials*, vol. 91, pp. 309-314, <https://doi.org/10.1016/j.jmbbm.2018.12.034>
- Antunes Junior, C, Mercuri, EGF, Franco, APG de O, Costa, M, Karam, LZ, Kalinowski, HJ & Gomes, OMM 2020, 'Bulk fill flow resin contraction using 3D finite element model and calibration by fiber Bragg grating measurement', *Computer Methods in Biomechanics and Biomedical Engineering*, vol. 23, no. 14, pp. 1127-1137, <https://doi.org/10.1080/10255842.2020.1789607>
- Ausiello, P, Ciaramella, S, Di Rienzo, A, Lanzotti, A, Ventre, M & Watts, DC 2019, 'Adhesive class I restorations in sound molar teeth incorporating combined resin-composite and glass ionomer materials: CAD-FE modeling and analysis', *Dental Materials*, vol. 35, no. 10, pp. 1514-1522, <https://doi.org/10.1016/j.dental.2019.07.017>
- Ausiello, P, Ciaramella, S, Garcia-Godoy, F, Martorelli, M, Sorrentino, R & Gloria, A 2017a, 'Stress distribution of bulk-fill resin composite in class II restorations', *American Journal of Dentistry*, vol. 30, no. 4, pp. 227-232
- Ausiello, P, Ciaramella, S, Martorelli, M, Lanzotti, A, Gloria, A & Watts, DC 2017b, 'CAD-FE modeling and analysis of class II restorations incorporating resin-composite, glass ionomer and glass ceramic materials', *Dental Materials*, vol. 33, no. 12, pp. 1456-1465, <https://doi.org/10.1016/j.dental.2017.10.010>
- Avçılar, İH & Bakır, Ş 2023, 'Use of fiber-containing materials in restorative dentistry', *Journal of Dental Sciences and Education*, vol. 1, no. 2, pp. 49-54, <https://doi.org/10.51271/jdse-0010>
- Boaro, LCC, Goncalves, F, Guimarães, TC, Ferracane, JL, Versluis, A & Braga, RR 2010, 'Polymerization stress, shrinkage and elastic modulus of current low-shrinkage restorative composites', *Dental Materials*, vol. 26, no. 12, pp. 1144-1150, <https://doi.org/10.1016/j.dental.2010.08.003>
- Chuang, SF, Chang, CH & Chen, TYF 2011, 'Contraction behaviors of dental composite restorations - Finite element investigation with DIC validation', *Journal of the Mechanical Behavior of Biomedical Materials*, vol. 4, no. 8, pp. 2138-2149, <https://doi.org/10.1016/j.jmbbm.2011.07.014>
- Dejak, B & Młotkowski, A 2015, 'A comparison of stresses in molar teeth restored with inlays and direct restorations, including polymerization shrinkage of composite resin and tooth loading during mastication', *Dental Materials*, vol. 31, no. 3, p. e77-e87, <https://doi.org/10.1016/j.dental.2014.11.016>

Ersen, KA, Gürbüz, Ö & Özcan, M 2020, 'Evaluation of polymerization shrinkage of bulk-fill resin composites using microcomputed tomography', *Clinical Oral Investigations*, vol. 24, no. 5, pp. 1687-1693, <https://doi.org/10.1007/s00784-019-03025-5>

Fennis, WMM, Kuijs, RH, Barink, M, Kreulen, CM, Verdonshot, N & Creugers, NHJ 2005, 'Can internal stresses explain the fracture resistance of cusp-replacing composite restorations?', *European Journal of Oral Sciences*, vol. 113, no. 5, pp. 443-448, <https://doi.org/10.1111/j.1600-0722.2005.00233.x>

Ferracane, JL & Hilton, TJ 2016, 'Polymerization stress - Is it clinically meaningful?', *Dental Materials*, vol. 32, no. 1, pp. 1-10, <https://doi.org/10.1016/j.dental.2015.06.020>

Ferracane, JL 2005, 'Developing a more complete understanding of stresses produced in dental composites during polymerization', *Dental Materials*, vol. 21, no. 1, pp. 36-42, <https://doi.org/10.1016/j.dental.2004.10.004>

Fok, A & Chew, HP 2020, *Mathematical models for dental materials research*, Springer, <https://doi.org/10.1007/978-3-030-37849-3>

Gallo, M, Abouelleil, H, Chenal, J, Adrien, J, Lachambre, J, Colon, P & Maire, E 2019, 'Polymerization shrinkage of resin-based composites for dental restorations: A digital volume correlation study', *Dental Materials: Official Publication of the Academy of Dental Materials*, <https://doi.org/10.1016/j.dental.2019.08.116>

Genisa, M, Shuib, S, Rajion, ZA, Mohamad, D & Arief, EM 2020, 'Dental implant monitoring using resonance frequency analysis (RFA) and cone beam computed tomography (CBCT) measurement', *International Journal of Technology*, vol. 11, no. 5, pp. 1015-1024, <https://doi.org/10.14716/ijtech.v11i5.4326>

Hamdy, TM 2021, 'Polymerization shrinkage in contemporary resin-based dental composites: A review article', *Egyptian Journal of Chemistry*, vol. 64, no. 6, pp. 3087-3092, <https://doi.org/10.21608/EJCHEM.2021.60131.3286>

Heck, K, Manhart, J, Hickel, R & Diegritz, C 2018, 'Clinical evaluation of the bulk fill composite QuiXfil in molar class I and II cavities: 10-year results of a RCT', *Dental Materials*, vol. 34, no. 6, pp. e138-e147, <https://doi.org/10.1016/j.dental.2018.03.023>

Ismail, NF, Islam, MS, Shuib, S, Ahmad, R & Shahmin, MA 2020, 'Influence of dental implant design on stress distribution and micromotion of mandibular bone', *Applied Mechanics and Materials*, vol. 899, pp. 81-93, <https://doi.org/10.4028/www.scientific.net/amm.899.81>

Kholil, A, Kiswanto, G, Al Farisi, A & Istiyanto, J 2023, 'Finite element analysis of lattice structure model with control volume manufactured using additive manufacturing', *International Journal of Technology*, vol. 14, no. 7, pp. 1428-1437, <https://doi.org/10.14716/ijtech.v14i7.6660>

Kim, RJY, Kim, YJ, Choi, NS & Lee, IB 2015, 'Polymerization shrinkage, modulus, and shrinkage stress related to tooth-restoration interfacial debonding in bulk-fill composites', *Journal of Dentistry*, vol. 43, no. 4, pp. 430-439, <https://doi.org/10.1016/j.jdent.2015.02.002>

Krishna Alla, R, Lakshmi Sanka, GSSJ, Saridena, DSN, AV, R, MAKV, R & Raju Mantena, S 2023, 'Fiber-reinforced composites in dentistry: Enhancing structural integrity and aesthetic appeal', *International Journal of Dental Materials*, vol. 5, no. 3, pp. 78-85, <https://doi.org/10.37983/ijdm.2023.5303>

Liu, Q, Li, J & Liu, J 2017, 'ParaView visualization of Abaqus output on the mechanical deformation of complex microstructures', *Computers and Geosciences*, vol. 99, pp. 135-144, <https://doi.org/10.1016/j.cageo.2016.11.008>

Magne, P 2007, 'Efficient 3D finite element analysis of dental restorative procedures using micro-CT data', *Dental Materials*, vol. 23, no. 5, pp. 539-548, <https://doi.org/10.1016/j.dental.2006.03.013>

Martinsen, M, El-Hajjar, RF & Berzins, DW 2013, '3D full field strain analysis of polymerization shrinkage in a dental composite', *Dental Materials*, vol. 29, no. 8, pp. e161-e167, <https://doi.org/10.1016/j.dental.2013.04.019>

Melo, MAS, Garcia, IM, Mokeem, L, Weir, MD, Xu, HHK, Montoya, C & Orrego, S 2023, 'Developing bioactive dental resins for restorative dentistry', *Journal of Dental Research*, vol. 102, no. 11, pp. 1180-1190, <https://doi.org/10.1177/00220345231182357>

- Mokhatar, SN & Abdullah, R 2012, 'Computational analysis of reinforced concrete slabs subjected to impact loads', *International Journal of Integrated Engineering*, vol. 4, no. 2, pp. 70-76
- Moraschini, V, Fai, CK, Alto, RM & Dos Santos, GO 2015, 'Amalgam and resin composite longevity of posterior restorations: A systematic review and meta-analysis', *Journal of Dentistry*, vol. 43, no. 9, pp. 1043-1050, <https://doi.org/10.1016/j.jdent.2015.06.005>
- Nagem Filho, H, Nagem, HD, Francisconi, PAS, Franco, EB, Mondelli, RFL & Coutinho, KQ 2007, 'Volumetric polymerization shrinkage of contemporary composite resins', *Journal of Applied Oral Science*, vol. 15, no. 5, pp. 448-452, <https://doi.org/10.1590/S1678-77572007000500014>
- Nayak, A, Jain, PK, Kankar, PK & Jain, N 2021, 'Effect of volumetric shrinkage of restorative materials on tooth structure: A finite element analysis', *Proceedings of the Institution of Mechanical Engineers, Part H: Journal of Engineering in Medicine*, vol. 235, no. 5, pp. 493-499, <https://doi.org/10.1177/0954411921990138>
- Norli, MHM, Sukimi, AKA, Ramlee, MH, Mahmud, J & Abdullah, AH 2024, 'Static structural analysis on different topology optimization transtibial prosthetic socket leg', *International Journal of Technology*, vol. 15, no. 2, pp. 455-462, <https://doi.org/10.14716/ijtech.v15i2.6711>
- Novaes, JB, Talma, E, Las Casas, EB, Aregawi, W, Kolstad, LW, Mantell, S, Wang, Y & Fok, A 2018, 'Can pulpal floor debonding be detected from occlusal surface displacement in composite restorations?', *Dental Materials*, vol. 34, no. 1, pp. 161-169, <https://doi.org/10.1016/j.dental.2017.11.019>
- Pereira, VA, Câmara, JVF, Prudêncio, AV, Serrano, LE, Barbosa, IF, Vianna, RFC, Campos, PRB, Castro, AN & Pereira, GDS 2020, 'Advanced polymerization system of photoinitiators in dental materials for aesthetic-functional restoration: Case report', *Research, Society and Development*, vol. 9, no. 9, article e890997984, <https://doi.org/10.33448/RSD-V9I9.7984>
- Rodrigues, FP, Silikas, N, Watts, DC & Ballester, RY 2012, 'Finite element analysis of bonded model class I restorations after shrinkage', *Dental Materials*, vol. 28, no. 2, pp. 123-132, <https://doi.org/10.1016/j.dental.2011.10.001>
- Sampaio, CS, Fernández Arias, J, Atria, PJ, Cáceres, E, Pardo Díaz, C, Freitas, AZ & Hirata, R 2019, 'Volumetric polymerization shrinkage and its comparison to internal adaptation in bulk fill and conventional composites: A μ CT and OCT in vitro analysis', *Dental Materials*, vol. 35, no. 11, pp. 1568-1575, <https://doi.org/10.1016/j.dental.2019.07.025>
- Siripath, N, Jantepa, N, Sucharitpwatskul, S & Suranuntchai, S 2024, 'Integrating Taguchi method and finite element modelling for precision ball joint manufacturing with AISI 1045 medium carbon steel', *International Journal of Technology*, vol. 15, no. 6, pp. 1801-1822, <https://doi.org/10.14716/ijtech.v15i6.7132>
- Soares, CJ, Faria-E-Silva, AL, Rodrigues, MP, Fernandes Vilela, AB, Pfeifer, CS, Tantbiroj, D & Versluis, A 2017, 'Polymerization shrinkage stress of composite resins and resin cements - What do we need to know?', *Brazilian Oral Research*, vol. 31, pp. 49-63, <https://doi.org/10.1590/1807-3107BOR-2017.vol31.0062>
- Versluis, A, Tantbiroj, D, Pintado, MR, DeLong, R & Douglas, WH 2004, 'Residual shrinkage stress distributions in molars after composite restoration', *Dental Materials*, vol. 20, no. 6, pp. 554-564, <https://doi.org/10.1016/j.dental.2003.05.007>
- Wang, Z & Chiang, MYM 2016, 'Correlation between polymerization shrinkage stress and C-factor depends upon cavity compliance', *Dental Materials*, vol. 32, no. 3, pp. 343-352, <https://doi.org/10.1016/j.dental.2015.11.003>
- Weinmann, W, Thalacker, C & Guggenberger, R 2005, 'Siloranes in dental composites', *Dental Materials*, vol. 21, no. 1, pp. 68-74, <https://doi.org/10.1016/j.dental.2004.10.007>